



OPEN ACCESS

EDITED BY

Yair Lotan,
University of Texas Southwestern
Medical Center, United States

REVIEWED BY

Timothy Clinton,
Harvard Medical School,
United States
Shengjie Chai,
Uber Technologies, Inc.,
United States

*CORRESPONDENCE

Wenjie Xie
xwjuro@sina.com

[†]These authors have contributed
equally to this work

SPECIALTY SECTION

This article was submitted to
Genitourinary Oncology,
a section of the journal
Frontiers in Oncology

RECEIVED 06 May 2022

ACCEPTED 31 October 2022

PUBLISHED 23 November 2022

CITATION

Luo L, Li F, Gong B, Xi P and Xie W
(2022) A novel prognostic model
based on cellular senescence-related
gene signature for bladder cancer.
Front. Oncol. 12:937951.
doi: 10.3389/fonc.2022.937951

COPYRIGHT

© 2022 Luo, Li, Gong, Xi and Xie. This is
an open-access article distributed under
the terms of the [Creative Commons
Attribution License \(CC BY\)](https://creativecommons.org/licenses/by/4.0/). The use,
distribution or reproduction in other
forums is permitted, provided the
original author(s) and the copyright
owner(s) are credited and that the
original publication in this journal is
cited, in accordance with accepted
academic practice. No use,
distribution or reproduction is
permitted which does not comply with
these terms.

A novel prognostic model based on cellular senescence- related gene signature for bladder cancer

Lianmin Luo^{1†}, Fenghua Li^{2†}, Binbin Gong^{1†}, Ping Xi¹
and Wenjie Xie^{1*}

¹Department of Urology, The First Affiliated Hospital of Nanchang University, Nanchang, Jiangxi, China, ²Department of Obstetrics and Gynecology, The First Affiliated Hospital of Nanchang University, Nanchang, Jiangxi, China

Background: Cellular senescence plays crucial role in the progression of tumors. However, the expression patterns and clinical significance of cellular senescence-related genes in bladder cancer (BCa) are still not clearly clarified. This study aimed to establish a prognosis model based on senescence-related genes in BCa.

Methods: The transcriptional profile data and clinical information of BCa were downloaded from TCGA and GEO databases. The least absolute shrinkage and selection operator (LASSO), univariate and multivariate Cox regression analyses were performed to develop a prognostic model in the TCGA cohort. The GSE13507 cohort were used for validation. Gene ontology (GO), Kyoto Encyclopedia of Genes and Genomes (KEGG), and single-sample gene set enrichment analysis (ssGSEA) were performed to investigate underlying mechanisms.

Results: A six-gene signature (CBX7, EPHA3, STK40, TGFB11, SREBF1, MYC) was constructed in the TCGA databases. Patients were classified into high risk and low risk group in terms of the median risk score. Survival analysis revealed that patients in the higher risk group presented significantly worse prognosis. Receiver operating characteristic (ROC) curve analysis verified the moderate predictive power of the risk model based on the six senescence-related genes signature. Further analysis indicated that the clinicopathological features analysis were significantly different between the two risk groups. As expected, the signature presented prognostic significance in the GSE13507 cohort. Functional analysis indicated that immune-related pathways activity, immune cell infiltration and immune-related function were different between two risk groups. In addition, risk score were positively correlated with multiple immunotherapy biomarkers.

Conclusion: Our study revealed that a novel model based on senescence-related genes could serve as a reliable predictor of survival for patients with BCa.

KEYWORDS

cellular senescence, bladder cancer, prognosis signature, immune infiltration, biomarkers

Introduction

Bladder cancer (BCa) is one of the most life-threatening cancer worldwide, with nearly 8,3730 new cases and 1,7200 deaths in the United States in 2021 according to cancer statistics (1). BCa ranges from non-muscle-invasive bladder carcinoma (NMIBC) and muscle invasive bladder carcinoma (MIBC) according to whether the tumors invades the muscle layer of the bladder (2). Despite undergoing radical cystectomy, nearly 50% of MIBC patients still have lethal metastatic recurrence, with the 5-year overall survival rate <50% (3). Therefore, it is crucial to explore the possible therapeutic target and novel prognostic biomarkers for improving the clinical outcome of patients in BCa to guide clinical practice.

Cellular senescence is a durable cell cycle arrest wherein cells fail to proliferate but remain metabolically active (4). Cellular senescence is a very complex stress response that manipulating several physiological and pathological processes, including embryogenesis (5), wound healing (6), tissue reprogramming (7) and ageing (8). In recent years, the complex relationship between cellular senescence and cancer has incited growing interest (9, 10). In cancer, senescence works as a potent inhibitor of cell cycle to suppress the proliferation of cancer cells in mammals (11, 12). Thus, because of its tumor-suppressive effects, therapy-induced senescence, such as cytotoxic chemotherapy or radiation, also can represent a therapeutic regimen for cancer (13, 14). Paradoxically, senescence cells can evade the immune system and accumulate in tissues and secrete a variety of pro-inflammatory and growth-stimulatory molecules, commonly referred to as the senescence-associated secretory phenotype (SASP) which is now recognized as a significant driver of tumor growth, relapse, and metastasis (15, 16). Consistent with this notion, mounting evidence demonstrated that cellular senescence can promote cancer initiation, invasion, and metastasis *via* the SASP that can act in autocrine and paracrine fashion to recruit proinflammatory cells that can modify the tumour microenvironment, which in turn can modulate tumour development (17, 18). In recent years, a growing studies have investigated gene expression patterns for risk stratification of patients and constructing survival prediction models in cancer (19, 20). However, the expression

patterns and the potential clinical prognosis value of senescence-related genes in BCa have not yet been systematically analyzed.

In the present study, a prognostic model was constructed based on the six senescence-related genes signature in the TCGA cohort. Then, we validated the predictive power of the model in the GEO cohort. Finally, functional enrichment analysis were performed to investigate the underlying mechanisms.

Materials and methods

Data and resources

The data of RNA-sequencing data (FPKM values) and corresponding clinical information of BCa were downloaded from TCGA database (<https://genomecancer.ucsc.edu>) as training cohort. Patients were excluded if one or more clinical characteristics were incomplete. Finally, a total of 406 patients were included from TCGA database. The GSE13507 was downloaded from the gene expression omnibus database (GEO: <https://www.ncbi.nlm.nih.gov/geo/>) as a validation cohort.

Identification of senescence-related differentially expressed genes

The list of senescence-related genes were collected from the CellAge database (Supplementary Table 1). The “limma” R package used to identify the senescence-related differentially expressed genes (DEGs) between tumor tissues and normal tissues based on the screening criteria of false discovery rate (FDR) < 0.05 and $|\log_2FC| > 1$.

Construction and validation of a prognostic senescence-related gene model

Univariate Cox regression analysis was used to screen senescence-related genes with prognostic values ($P < 0.05$). The Least Absolute Shrinkage and Selection Operator (LASSO) regression with “glmnet” R package was applied in

order to avoid overfitting. Subsequently, the candidate genes selected into multivariate Cox regression analysis in order to determine final prognostic senescence-related genes. Finally, the risk score of each samples was calculated based on the amount of senescence-related genes expression and corresponding coefficients. The calculation formula was as follows: risk score = $\beta_{mRNA1} \times \text{Expression}_{mRNA1} + \beta_{mRNA2} \times \text{Expression}_{mRNA2} + \beta_{mRNA3} \times \text{Expression}_{mRNA3} + \dots + \beta_{mRNA_n} \times \text{Expression}_{mRNA_n}$.

The patients were classified into high risk and low risk group based on the median value of the risk score. Kaplan-Meier analysis was performed to compare the overall survival between high risk and low risk group. The receiver operating characteristic (ROC) curve analysis was used to evaluate the predictive accuracy of the senescence-related genes signature.

Parameters including age, gender, grade, TNM staging system, stage, and risk score were analyzed by univariate analysis. The candidate parameters $p < 0.05$ in univariate analysis selected into multivariate analysis in order to determine independent prognostic factors.

Comprehensive analysis of the prognostic model

Parameters including age, gender, grade, TNM staging system, stage, and risk score were analyzed by univariate analysis. The candidate parameters $P < 0.05$ in univariate analysis selected into multivariate analysis in order to determine independent prognostic factors.

To further investigate the correlations between the two risk groups, clinical variables and senescence-related genes, we compared the differences in age, gender, grade, TNM staging system, stage, and senescence-related genes between the high risk and low risk group. The results were displayed as a heatmap.

Functional and pathway enrichment analysis

The “limma” R package was applied to analyze the DEGs between the high risk and low risk group based on the screening criteria of false discovery rate (FDR) < 0.05 and $|\log_2FC| > 1$. Gene Ontology (GO) analysis and Kyoto Encyclopedia of Genes and Genomes (KEGG) pathway analysis were conducted to identify the biological functions and the signaling pathways that were associated with the DEGs.

Depicting immune infiltration characteristics

Single-sample gene set enrichment analysis (ssGSEA) was used to estimate the infiltrating scores of the 16 immune cells

subsets and 13 immune-related pathways between the high risk and low risk groups.

Evaluation of inflammatory response-related genes characteristics and EMT phenotype

Inflammatory response-related genes were downloaded from the Molecular Signatures Database (MSigDB) (Supplementary Table 1) and compared between the high risk and low risk groups. The epithelial-to-mesenchymal transition (EMT) phenotype was evaluated based on the expression of EMT marker genes including SNAI1, SNAI2, ZEB1, ZEB2, TWIST1, Vimentin, Fibronectin, N-cadherin, and E-cadherin.

RNA extraction and quantitative real-time PCR analysis

Total RNA was extracted from 5 paired human BCa tissues and adjacent non-tumorous tissues using TRIzol Reagent (Invitrogen). The reverse transcription was conducted with PrimeScriptTM RT reagent Kit (TaKaRa). Q-PCR was done with SYBR green Premix Ex Taq II (Takara). GAPDH was selected as an internal control. The sequence of primers were listed in Supplementary Table 2.

Statistical analysis

The statistical analyses were performed using the R software (Version R-4.1.2) and GraphPad Prism 8.0. Student's t-test was applied to compare the difference between binary groups with continuous variables. $P < 0.05$ was considered statistically significant. P values were showed as: ns, not significant; *, $P < 0.05$; **, $P < 0.01$; ***, $P < 0.001$.

Results

Identification of prognostic cellular senescence-related gene of bladder cancer in the TCGA cohort

The flow diagram of the study is presented in Figure 1. Among 278 cellular senescence-related genes, 47 were differentially expressed between tumor samples and normal samples, including 24 downregulated genes and 23 upregulated genes (Figures 2A, B). Through univariate Cox regression analysis, we identified 13 prognostic cellular senescence-related genes associated with overall survival, as detailed in Figure 2C.

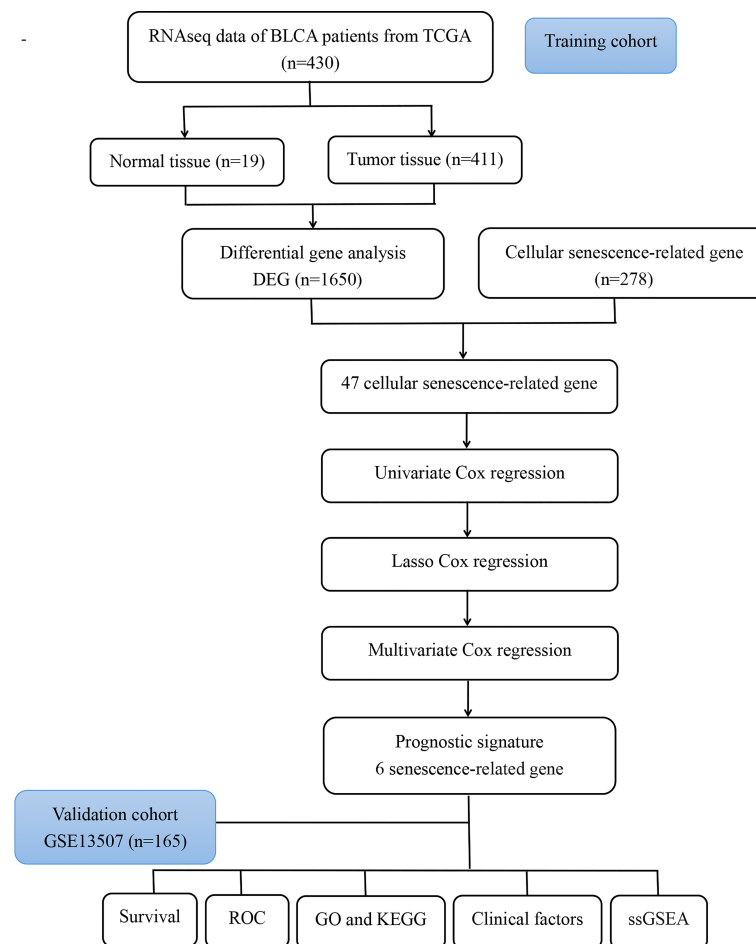


FIGURE 1
Flow chart of the analysis process in our study.

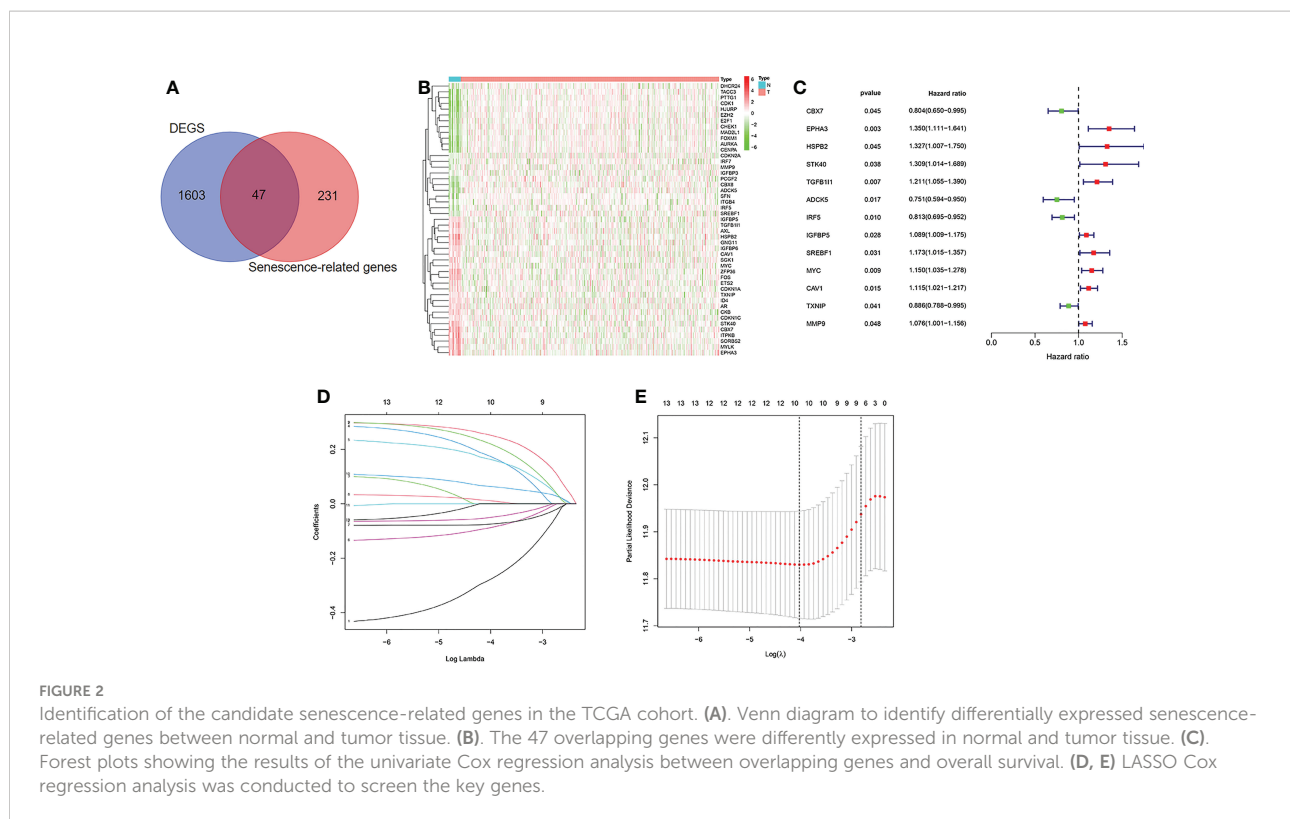
Construction of a prognostic model in the training cohort

LASSO Cox regression analysis was conducted to screen the key genes among the cellular senescence-related genes based on univariate Cox regression analysis results (Figures 2D, E). Then, ten genes were selected into multivariate Cox regression analysis according to the optimal value of λ . Finally, six genes signature, namely, CBX7, EPHA3, STK40, TGFB111, SREBF1, and MYC, was constructed. The risk score of each patient was calculated according to the following formula: risk score = $(-0.474 \times$ the expression level of CBX7) + $(0.354 \times$ the expression level of EPHA3) + $(0.283 \times$ the expression level of STK40) + $(0.244 \times$ the expression level of TGFB111) + $(0.287 \times$ the expression level of SREBF1) + $(0.104 \times$ the expression level of MYC). Patients were stratified into high risk group (n=203) and low risk group (n=203) based on the median risk score. As shown in Figures 3A, B, patients in the high risk group had higher

probability of death than that in the low risk group. Patients in the high risk group had high expression of EPHA3, TGFB111, STK40, SREBF1, and MYC but low expression of CBX7 (Figure 3C). The Kaplan-Meier analysis demonstrated that patients in the high risk group had significantly poorer overall survival (OS) than those in the low risk group (Figure 3D). The ROC curves was conducted to evaluate the predictive accuracy of the risk model for OS. The results demonstrated that the area under ROC curve (AUC) reached 0.671 at 3 year and 0.708 at 5 year (Figure 3E).

Validation of the prognostic risk model in the validation cohort

To evaluate whether the risk model constructed from the TCGA cohort was robust, the patients from the GSE13507 were categorized into high risk group and low risk group according to



the median value calculated with the same formula as the training cohort. Similar to the results obtained from the training cohort, patients in the high risk group of validation cohort were more likely to encounter a higher probability of death (Figures 3F, G). Likewise, patients in the high risk group had high expression of EPHA3, TGFB111, STK40, SREBF1, and MYC but low expression of CBX7 (Figure 3H). As expected, patients exhibited worse OS in the high risk group. (Figure 3I). The AUC value reached 0.703 at 3 year, 0.691 at 5 years (Figure 3J).

Correlation between the cellular senescence-related gene signature model and the clinicopathological features

To evaluate whether the prognostic model based on cellular senescence-related gene was an independent risk factor for OS, the Cox regression analysis was performed. The results obtained from univariate Cox regression analysis indicated that the risk score was significantly correlated with OS in the training cohort (HR 1.651, 95% CI:1.437–1.898, $P < 0.001$) and validation cohort (HR 1.562, 95% CI: 1.095–2.226, $P = 0.014$) (Figures 4A, C). Multivariate Cox regression demonstrated that riskScore (HR 1.513, 95% CI 1.303–1.757, $P < 0.001$) would be an independent

risk factors for OS in the training cohort (Figure 4B), however, the result was not observed in the validation cohort (Figure 4D).

Subsequently, the relevance between the risk score and clinicopathological parameters of patients was evaluated and exhibited as a heatmap in the training cohort (Figure 4E) and validation cohort (Figures 4G). The results confirmed that the risk score had strong correlations with the tumor grade, N stage, T stage and TNM stage in the training cohort (Figure 4F). The similar results were observed from the validation cohort (Figure 4H). All these results verified that as the risk score increased, the probability of progressing to a later clinical phenotypes gradually increased, suggesting that cellular senescence-related gene signature would be a valuable cancer prognostic model in the progression of BCa.

Analysis expression of the genes from the signature in bladder cancer patients

We detected mRNA expression of the genes from this signature in 5 paired human BCa tissues and adjacent normal tissues. The results indicated that the expression of EPHA3, TGFB111, STK40 and CBX7 were down-regulated in BCa tissues than that in adjacent normal tissues. The expression of SREBF1 and MYC were up-regulated in BCa tissues than that in adjacent normal tissues (Supplementary Figure 1).

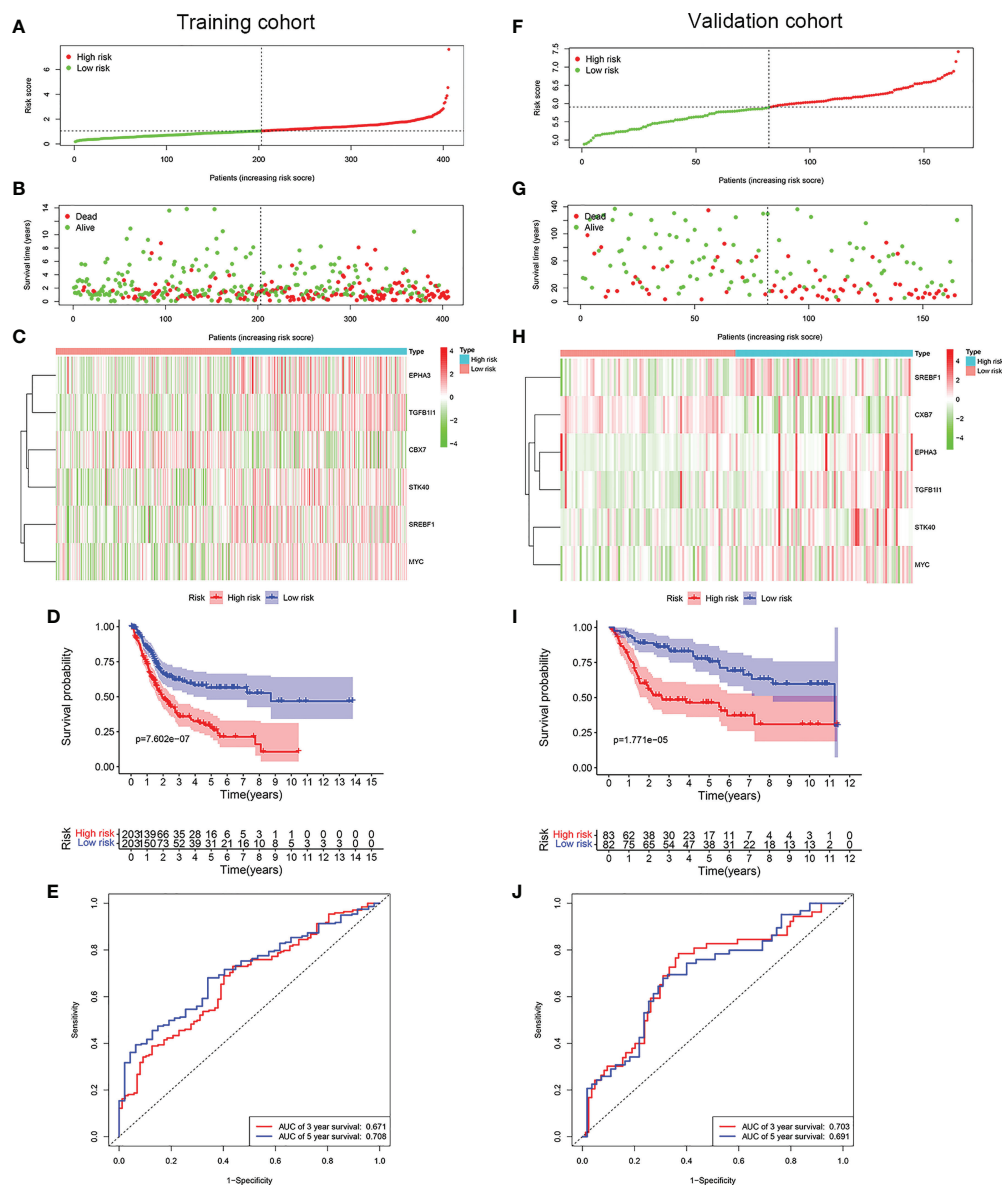


FIGURE 3 Construction of a prognostic model of senescence-related genes in the TCGA cohort and validation in GSE13507 cohort. (A) Distribution of patients' risk scores, (B) survival status, (C) Prognostic signature signal heatmap, (D) Kaplan-Meier curves for the overall survival, and (E) ROC curve of the prognostic signature in the TCGA cohort. (F) Distribution of patients' risk scores, (G) survival status, (H) Prognostic signature signal heatmaps, (I) Kaplan-Meier curves for the overall survival, and (J) ROC curve of the prognostic signature in the GSE13507 cohort.

Functional enrichment analyses in training cohort

To investigate underlying biological functions and pathways that were related to the risk score, the GO enrichment and KEGG pathway analyses were performed using the DEGs between the high risk group and low risk group. The GO analysis results demonstrated that the biological process (BP) of DEGs mainly focused on

extracellular matrix organization, extracellular structure organization, humoral immune response, regulation of cellular response to growth factor, and so on (Figures 5A, B). KEGG pathway analysis revealed that DEGs were significantly enriched in PI3K-Akt signaling pathway, Proteoglycans in cancer, ECM-receptor interaction, AGE-RAGE signaling pathway, Transcriptional misregulation in cancer, TGF-beta signaling pathway, Bladder cancer, IL-17 signaling pathway (Figures 5C, D).

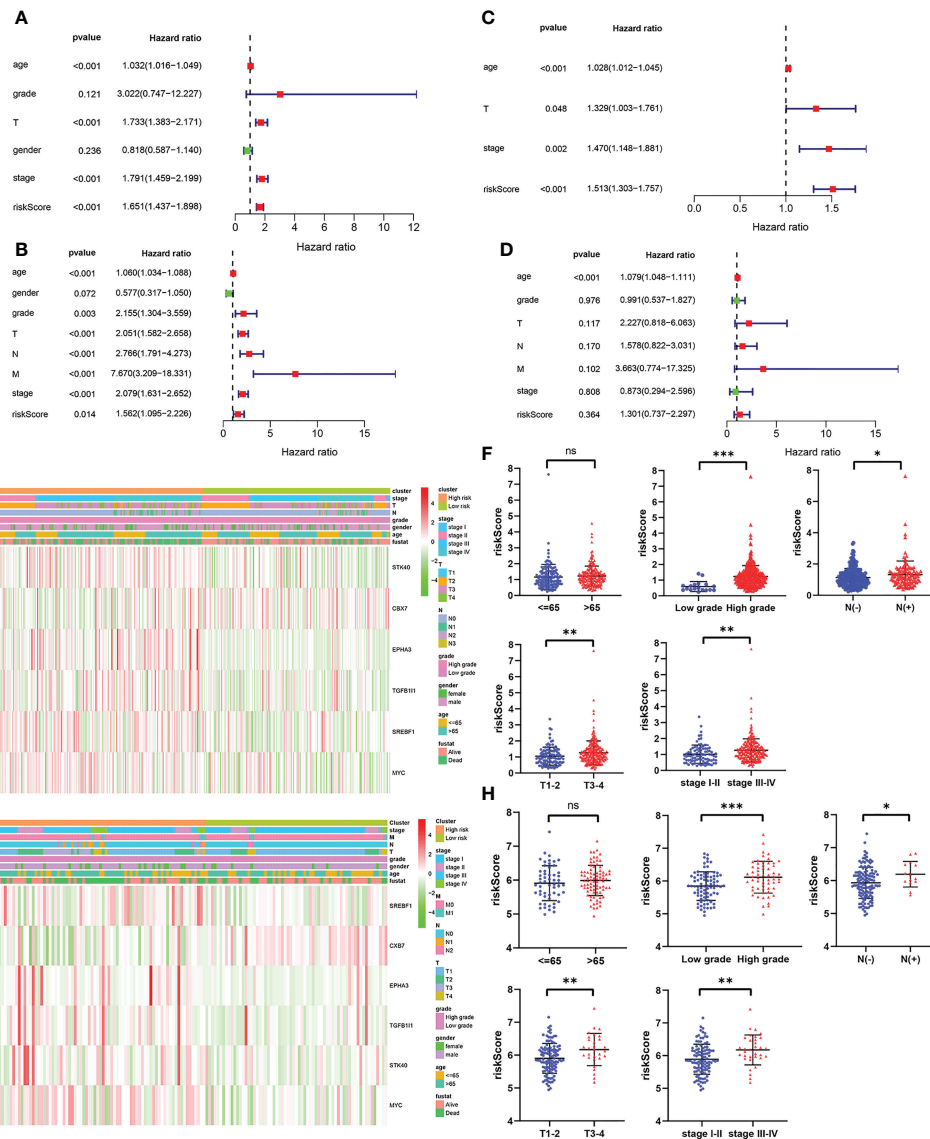
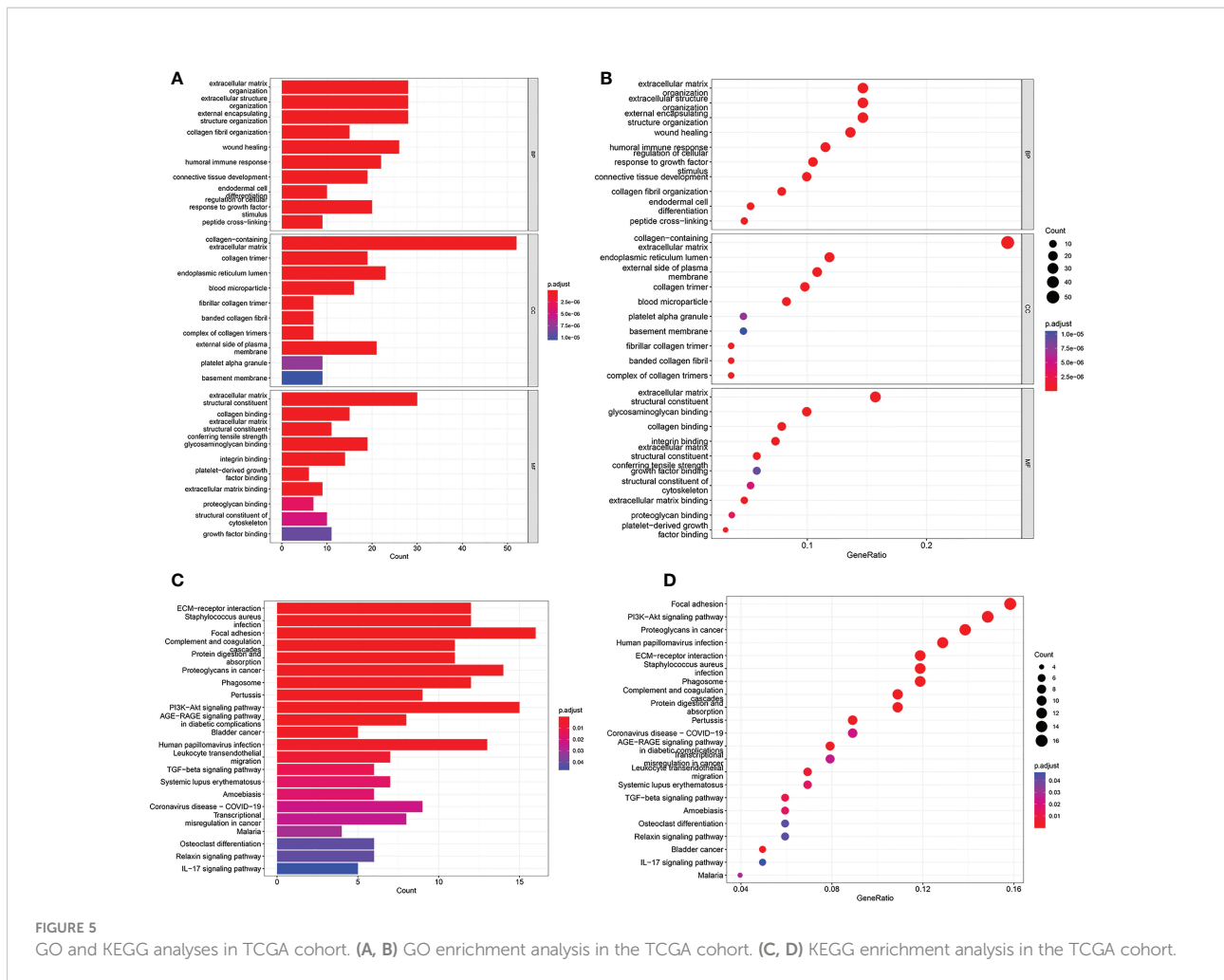


FIGURE 4 The independent prognostic factors for overall survival. (A, B) Univariate and multivariate cox regression of prognostic factors in the TCGA cohort. (C, D) Univariate and multivariate cox regression of prognostic factors in the GSE13507 cohort. (E, F) The relationship between risk score and clinicopathological parameters in the TCGA cohort. (G, H) The relationship between risk score and clinicopathological parameters in the GSE13507 cohort. P values were showed as: ns, not significant; *, $P < 0.05$; **, $P < 0.01$; ***, $P < 0.001$.

Differential immune infiltration characteristics landscape

To evaluate the correlation between the risk score and immune activity, the ssGSEA algorithm was performed for the purpose of calculating the infiltrating scores of the different immune cell subsets, as well as immune-related function. The scores of Treg, TIL, Th2_cells, Th1_cell, Tfh, T_helper_cells, pDCs, Neutrophils, Mast_cells, Macrophages, iDCs, DCs, CD

+ T_cells, B_cells and aDCs were significantly higher in high risk group than that in the low risk group in the training cohort (Figures 6A, B), suggesting immune cell abundance was significantly correlated with the riskScore. In addition, as shown in Figure 6C, the scores of immune function in the high risk group was stronger than that in the low risk group. Interestingly, the scores of Th1_cell, Tfh, T_helper_cells, pDCs, Neutrophils, Macrophages, DCs, and aDCs were significantly higher in the high risk group than that in the low risk group in

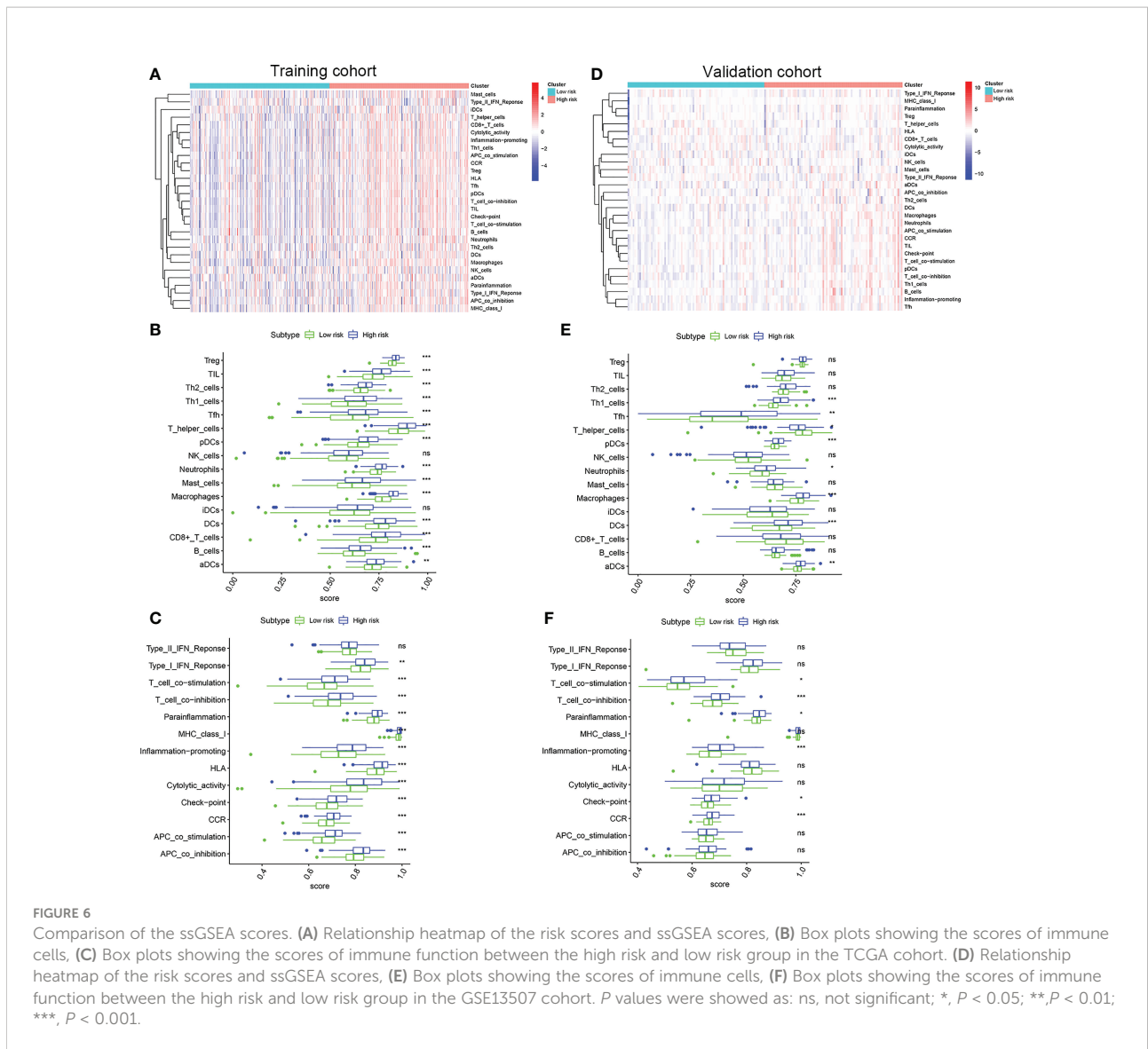


validation cohort (Figures 6D, E). Moreover, compared with the low risk group, the scores of T_{cell}_co-stimulation, T_{cell}_co-inhibition, Inflammation-promoting, Check-point, CCR were significantly higher in the high risk group (Figure 6F). All these results, together, confirmed that the risk score had strong correlations with immune cell infiltration and immune-related function.

Considering the important role of immune checkpoint molecules such as PD-1, PD-L1, LAG3 and CTLA-4 in tumor immune microenvironment, the expression levels of these molecules were explored between two groups. Interestingly, PD-1, PD-L1, LAG3 and CTLA-4 of the high risk group were highly expressed in the training cohort (Figures 7A, B). In addition, we utilized validation cohort for exploring the molecules expression levels. Results presented that although the expression of PD-1 was no statistical difference, PD-L1, LAG3 and CTLA-4 were significantly high in the high risk group (Figures 7C, D).

Differences in inflammatory response-related genes characteristics and EMT phenotype between high and low risk group

Due to the close connection between the senescence-associated secretory phenotype (SASP) and inflammatory response and epithelial mesenchymal transition (EMT), we decided to further investigate the differences in inflammatory response-related genes characteristics and EMT phenotype between two groups. First, The inflammatory response-related DEGs were identified between two groups by the “limma” R package based on the screening criteria of false discovery rate (FDR) < 0.05 and |log₂FC| > 1. We found that these inflammatory response-related DEGs were highly expressed in high risk group and lowly expressed in low risk group in training cohort (Figure 8A). The similar results were observed from the validation cohort (Figure 8B). Next, EMT hallmark genes

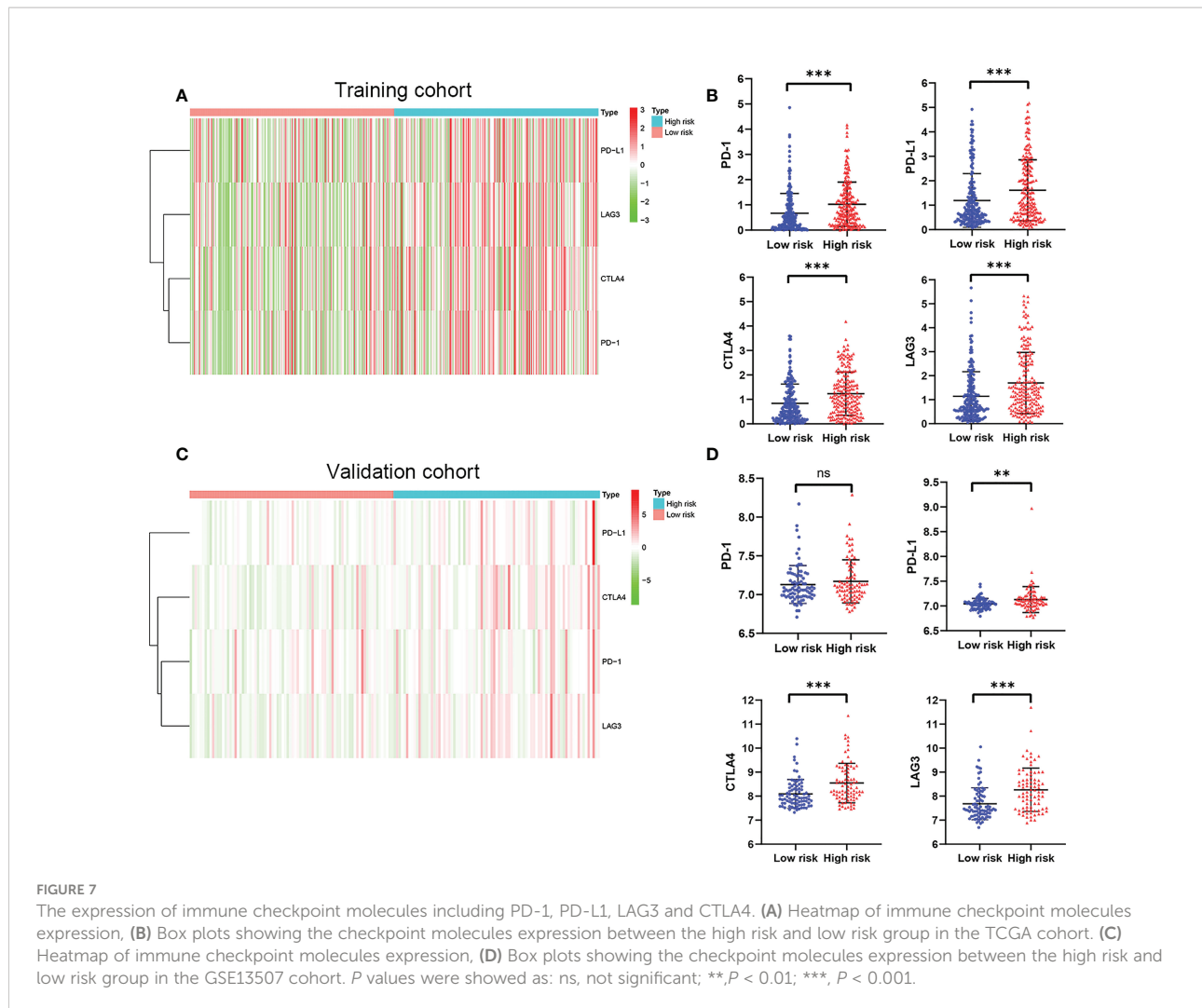


expression were explored between high and low risk group. As illustrated in **Figures 8C, D**, significantly higher expression of EMT hallmark genes including *SNAI2*, *N-cadherin*, *Vimentin*, *ZEB1*, *ZEB2*, *SNAI1*, *Fibronectin* and *TWIST1* were observed in high risk group in the training cohort, along with the low expression of *E-cadherin*, suggesting that risk score was positively correlated with cell EMT pathway. Subsequently, these genes expression levels were explored in validation cohort. Results presented that although the expression of *ZEB1*, *SNAI2* and *E-cadherin* were no statistical difference, *ZEB2*, *TWIST1*, *SNAI1*, *Fibronectin* and *N-cadherin* were significantly higher in the high risk group (**Figures 8E, F**), which was in accordance with our results that risk score was positively correlated with cell EMT pathway.

Discussion

Bca is an extremely frequent genitourinary malignancy. Despite the therapeutic strategies and individualized therapies improvement, a significant proportion of patients with muscle invasive bladder carcinoma (MIBC) undergoing radical cystectomy still experience local recurrence and distant metastasis. Unfortunately, effective clinical treatments for these patients are relatively limited. Therefore, it is of great importance to identify novel molecular biomarkers to better advance cancer therapies and predict the prognostic of patients with Bca.

Cellular senescence is a state of durable growth arrest induced by various stresses (21). Several common features of cellular senescence include high expression of the cell cycle



inhibitor p16^{Ink4a}, and a distinctive senescence-associated secretory phenotype (SASP) that involves cytokines, chemokines, matrix metalloproteinases, growth factors and angiogenic factors (22). Emerging evidence has shown that cellular senescence plays a crucial role in tumor microenvironment (TME) and tumor growth (23, 24). In this study, the prognostic signature was constructed based on senescence-related genes in the TCGA cohort. Then, we validated the predictive power of the model in the GSE13507 cohort. The vast majority of patients in the TCGA are MIBC. The GSE13507 dataset include 101 NMIBC and 62 MIBC. Finally, six genes, including CBX7, EPHA3, STK40, TGFB111, SREBF1, and MYC were filtered out to construct the prognostic model.

CBX7 (Chromobox protein homolog 7) is reported to belong to the Chromobox protein family (25). Previous studies revealed that CBX7 expression was down-regulated in multiple human carcinomas and the loss of CBX7 expression was associated with increasing malignancy (26, 27). A recent study indicated that

CBX7 acted as a tumor suppressor in BCa and could suppress cancer cell aggressiveness by inhibiting ERK signaling (25). EPHA3 is a member of the Eph receptor tyrosine kinases and can bind cell membrane ligands to mediate cell communication regulate biological function, including tumour growth, angiogenesis and metastasis (28). EPHA3 is one of the potential anticancer targets, with up-regulation and tumor-promoting roles in a range of human cancers (29). However, the expression pattern and function of EPHA3 in BCa remains unclear, and further exploration are needed. STK40 (Serine/threonine kinase 40), also known as SHIK, which had been confirmed as a negative regulator of NF- κ B transcription (30).

A recent evidence displayed that STK40 acted as a tumor inhibitor in patients with Triple-negative breast cancers (31). The expression details and functions of STK40 in various cancer types still warrants further investigation. TGFB111, a scaffold protein, is also known as HIC-5, which can be expressed under the induction of TGF- β and hydrogen peroxide (32). Previous studies revealed that TGFB111 acted as key roles in a variety of

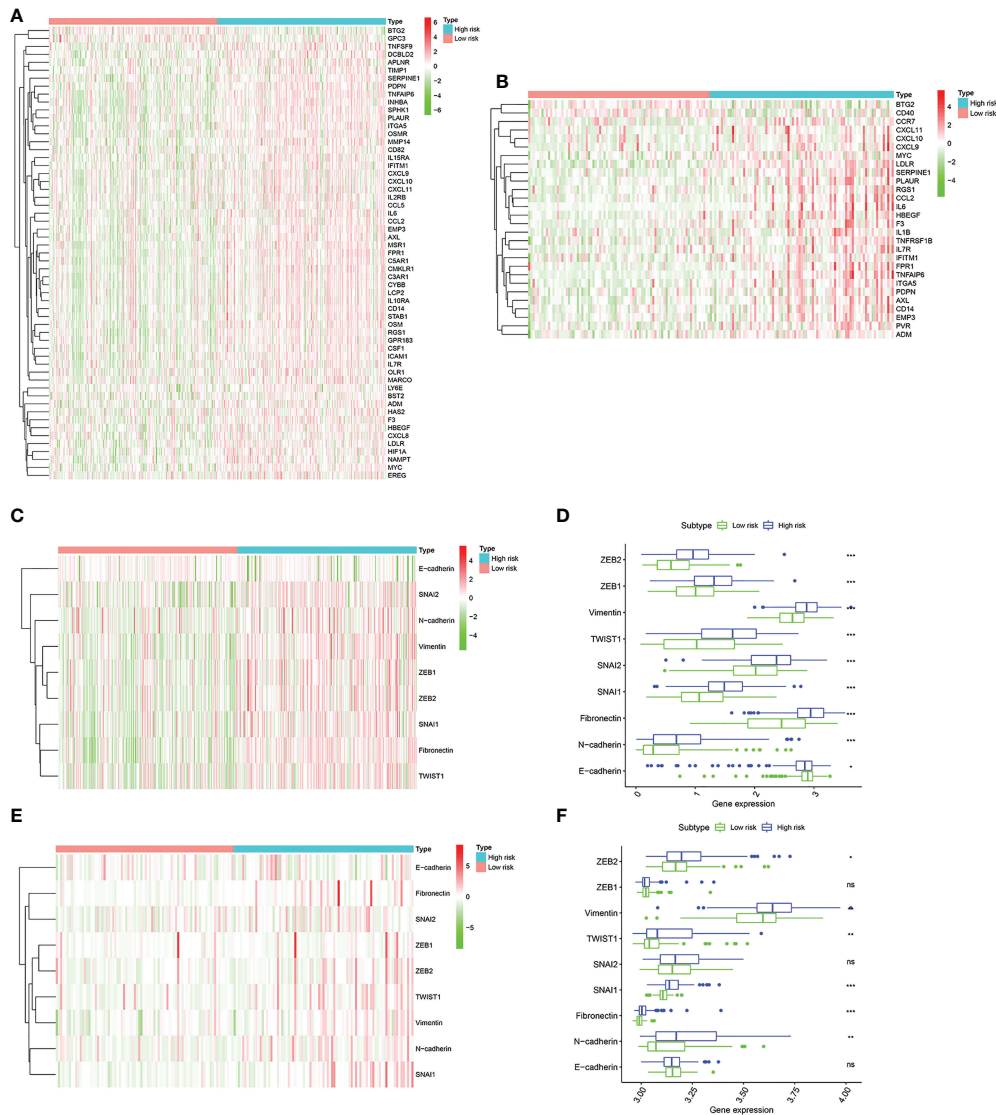


FIGURE 8

The landscape of inflammatory response-related genes and EMT hallmark genes including SNAI1, SNAI2, ZEB1, ZEB2, TWIST1, Vimentin, Fibronectin, N-cadherin, and E-cadherin. (A) Heatmap of inflammatory response-related DEGs expression between the high risk and low risk group in the TCGA cohort. (B) Heatmap of inflammatory response-related DEGs expression between the high risk and low risk group in the GSE13507 cohort. (C) Heatmap of EMT hallmark genes expression, (D) Box plots showing the EMT hallmark genes expression between the high risk and low risk group in the TCGA cohort. (E) Heatmap of EMT hallmark genes expression. (F) Box plots showing the EMT hallmark genes expression between the high risk and low risk group in the GSE13507 cohort. *P* values were showed as: ns, not significant; *, *P* < 0.05; **, *P* < 0.01; ***, *P* < 0.001.

pathological processes, including liver fibrosis (32), atherosclerosis (33), tumorigenesis and progression (34). TGFBI1 has been verified to be acted as an oncogene in several cancers, including esophageal squamous cell carcinoma (35), breast tumor (36), ovarian cancer (37), and osteosarcoma (38). SREBP1, a well-recognized transcriptional regulator of lipid metabolism (39). Previous studies have verified high expression of SREBP1 was related with a poor prognosis in multiple human tumors (40–42). MYC, one of the most

frequently investigated proto-oncogene, has been reported as one of the most highly amplified oncogene contributes to the initiation and development of many human cancers (43, 44). A recent study revealed that MYC inhibitor not only suppressed tumor growth in mice, but also increased T cell immune infiltration, enhanced PD-L1 expression on tumors, and increased tumor sensitivity to anti-PD1 immunotherapy (45).

The patients were divided into high risk and low risk group based on the median risk score. Compared to the low risk group,

patients in the high risk group had a higher probability of death. Survival analyses indicated that patients with high risk had a significantly poor prognosis. ROC curves indicated that higher consistency was existed between actual and predicted survival rate. Consistently, the percentage of patients with worse malignant phenotype, such as higher tumor grade, lymph node metastasis, and advanced TNM stage, was significantly higher in the high risk group.

We further reproduce the model in validation cohort to confirm the robustness of the risk model. As expected, results revealed that patients in the high risk group had a significantly increased risk of poor prognosis than that in the low risk group, which were consistent with our previous results. GO and KEGG analysis were performed based on DEGs between different risk groups to investigate the biological processes and signaling pathways that were related to the risk score. The results presented that DEGs were significantly enriched in extracellular matrix organization, humoral immune response, regulation of cellular response to growth factor, PI3K-Akt signaling pathway, TGF-beta signaling pathway, Bladder cancer, IL-17 signaling pathway. These biological processes are involved in immune biological processes and pathways (46–49). The extracellular matrix (ECM) is a combination of proteins and proteoglycans with structural and functional roles (50). Proteases and matrix metalloproteinases (MMPs) participate in ECM remodelling. Many evidence indicated that MMPs, such as MMP-7, MMP-10, associated with the progression in patients with BCa (51, 52). BCa is an immunogenic. Numerous studies found the influence of the immune microenvironment on BCa development and immunotherapy was applied for the treatment of BCa (53, 54). The development and progression of BCa has been associated with abnormal expression of a number of genes or aberrant activation of signaling pathways. Among them, PI3K-Akt pathway abnormally activated is crucial for BCa progression (55). Ruan et al. reported that inhibition of PI3K-Akt pathway significantly inhibited migration and invasion of BCa cells (56). TGF- β expression is up-regulated in tumor cells and TGF- β signaling pathway was notably associated with several hallmarks of cancer, such activating invasion and metastasis, inducing angiogenesis and drug resistance (57). Chen et al. found that TGF- β facilitated BCa cell proliferation, migration and invasion both *in vitro* and *in vivo* by inducing EMT (58). Liang et al. reported that ablation of TGF- β signaling suppressed the BCa cell proliferation and EMT, hence inhibited BCa progression in a BCa mouse model (59). The IL-17 cytokine family includes six ligands (IL-17A to IL-17F) and five receptors (IL-17RA to IL-17RE) (60). Previous study indicated that IL-17F protein served as an oncogene in BCa (61). IL-17A levels were significantly elevated in peripheral blood in patients with BCa than that in healthy control (62). Wang et al. found that IL-17A facilitated BCa growth in animal experiments (63).

BCa is considered as an immune cell infiltrating tumor. At present, many immune checkpoint inhibitors, including atezolizumab, durvalumab, nivolumab, pembrolizumab, and avelumab, have been approved by FDA for the treatment of advanced urothelial carcinoma (64–70). In this study, two risk group confirmed by us had significantly different immune characteristics. High risk group had a significantly correlated with higher infiltrating scores of immune-cell and immunity-related pathways. Moreover, the expression of immune checkpoint molecules including PD-1, PD-L1, LAG3, and CTLA4 was significantly higher in the high risk group in training cohort. Similar to this results, in the validation cohort, the patients with high risk had a significantly higher expression of PD-L1, LAG3, and CTLA4. These results suggested that patients in the high risk group may have a more favorable response to immune checkpoint inhibitor therapy than that in the low risk group.

Inflammation were widely involved in the tumorigenesis and progression of tumor, immune escape, and tumor microenvironment formation (71, 72). We further investigated the inflammatory response-related genes (IRGs) expression abundance between the high risk and the low risk group. It is found that most of the differentially expressed IRGs were significantly higher expression in the high risk group than that in the low risk group. Moreover, based on the expression of EMT hallmark genes including SNAI2, N-cadherin, Vimentin, ZEB1, ZEB2, SNAI1, Fibronectin, TWIST1 and E-cadherin, we found that patients with high risk score distinctly exhibited a mesenchymal phenotype, suggesting a higher tumor malignancy.

In our study, six genes signature, namely, CBX7, EPHA3, STK40, TGFBI1, SREBF1, and MYC, was constructed. Sun et al. identified a four-cell-senescence-regulator-gene prognostic index to predict the prognosis of patients with BCa (73). These four genes were PSMD14, PSMB5, PRPF19 and TPR. Zhou et al. developed an 8 immunosenescence-related gene pair signature to evaluate the overall survival of patients with BCa (74). These 8-gene pair were EGFR|MAPK1, TFRC|IRF1, ADIPOR2|GBP2, CTSS|THBS1, GBP2|CCN2, PSMD11|SRC, KIR2DL4|NOX4, and MAP2K1|ELAVL1. In TCGA cohort and GSE13507 cohort, we found that the high risk group and low risk group identified using cellular senescence-related gene in our study is not similar to the high risk group and low risk group identified in the Sun et al. and Zhou et al. papers (Supplementary Tables 3 and 4).

The risk score using gene signatures proposed in the Sun et al. and Zhou et al. papers were calculated. In TCGA cohort, the risk score calculated using gene signature proposed in our paper is not highly correlated with the risk score calculated using gene signatures proposed in the Sun et al. paper ($r=0.282$) and Zhou et al. papers ($r=0.135$). In GSE13507 cohort, the risk score

calculated using gene signature proposed in our paper is not highly correlated with the risk score calculated using gene signatures proposed in the Sun et al. paper ($r=0.115$) and Zhou et al. paper ($r=0.552$) (Supplementary Figure 2). Therefore, the prognostic gene signature proposed in our study has uniqueness and novelty.

Some limitations should be acknowledged in our study. First, data from the BCa cohort in our clinical center are incomplete, thus, we cannot use our own BCa cohort to validate the predictive power of the model. We will improve the clinical data in the future to further validate the predictive power of the model. Second, as our prognostic model was constructed and validated with retrospective data, a multi-center prospective study with larger population is required to confirm the clinical value of the model. Third, further experimental studies are needed to clarify the biological regulatory mechanisms of cellular senescence-related genes in the progression of BCa.

Conclusion

In summary, we established a novel prognostic model for BCa based on cellular senescence-related genes. Moreover, the model is capable of providing a reliable predictor for OS, clinical characteristics, and immune infiltration, which can serve as a valuable biomarker for bladder prognosis and progression.

Data availability statement

The raw data supporting the conclusions of this article will be made available by the authors, without undue reservation.

Ethics statement

The study was conducted in accordance with the Declaration of Helsinki, and the protocol was approved by the Ethics Committee of the First Affiliated Hospital of Nanchang University. The use of all samples was approved by the ethics committee, and informed consent was obtained from all enrolled patients.

References

1. Siegel RL, Miller KD, Fuchs HE, Jemal A. Cancer statistics, 2021. *CA Cancer J Clin* (2021) 71(1):7–33. doi: 10.3322/caac.21654
2. Sanli O, Dobruch J, Knowles MA, Burger M, Alemezaffar M, Nielsen ME, et al. Bladder cancer. *Nat Rev Dis Primers* (2017) 3:17022. doi: 10.1038/nrdp.2017.22

Author contributions

LL and WX were responsible for the study design and writing. BG was mainly responsible for data analysis, and FL and PX was mainly responsible for data collection. LL and WX was responsible for manuscript review and providing constructive comments. All authors read and approved the final manuscript. All authors contributed to the article and approved the submitted version.

Acknowledgments

We thank for using TCGA and GEO database for free.

Conflict of interest

The authors declare that the research was conducted in the absence of any commercial or financial relationships that could be construed as a potential conflict of interest.

Publisher's note

All claims expressed in this article are solely those of the authors and do not necessarily represent those of their affiliated organizations, or those of the publisher, the editors and the reviewers. Any product that may be evaluated in this article, or claim that may be made by its manufacturer, is not guaranteed or endorsed by the publisher.

Supplementary material

The Supplementary Material for this article can be found online at: <https://www.frontiersin.org/articles/10.3389/fonc.2022.937951/full#supplementary-material>

SUPPLEMENTARY FIGURE 1

Analysis expression of the genes from the signature in BCa patients.

SUPPLEMENTARY FIGURE 2

Analysis correlation of risk score between different studies.

3. Rouprêt M, Babjuk M, Burger M, Capoun O, Cohen D, Comperat EM, et al. European Association of urology guidelines on upper urinary tract urothelial carcinoma: 2020 update. *Eur Urol* (2021) 79:62–79. doi: 10.1016/j.eururo.2020.05.042
4. Rodier F, Campisi J. Four faces of cellular senescence. *J Cell Biol* (2011) 192:547–56. doi: 10.1083/jcb.201009094

5. Storer M, Mas A, Robert-Moreno A, Pecoraro M, Ortells MC, Di Giacomo V, et al. Senescence is a developmental mechanism that contributes to embryonic growth and patterning. *Cell* (2013) 155:1119–30. doi: 10.1016/j.cell.2013.10.041
6. Demaria M, Ohtani N, Youssef SA, Rodier F, Toussaint W, Mitchell JR, et al. An essential role for senescent cells in optimal wound healing through secretion of PDGF-AA. *Dev Cell* (2014) 31:722–33. doi: 10.1016/j.devcel.2014.11.012
7. Mosteiro L, Pantoja C, Alcazar N, Marion RM, Chondronasiou D, Rovira M, et al. Tissue damage and senescence provide critical signals for cellular reprogramming *in vivo*. *Science* (2016) 354:aaf4445. doi: 10.1126/science.aaf4445
8. Di Micco R, Krizhanovsky V, Baker D, d'Adda di Fagnana F. Cellular senescence in ageing: from mechanisms to therapeutic opportunities. *Nat Rev Mol Cell Biol* (2021) 22(2):75–95. doi: 10.1038/s41580-020-00314-w
9. Loo TM, Miyata K, Tanaka Y, Takahashi A. Cellular senescence and senescence-associated secretory phenotype *via* the cGAS-STING signaling pathway in cancer. *Cancer Sci* (2020) 111(2):304–11. doi: 10.1111/cas.14266
10. Milanovic M, Fan DNY, Belenki D, Däbritz JHM, Zhao Z, Yu Y, et al. Senescence-associated reprogramming promotes cancer stemness. *Nature* (2018) 553(7686):96–100. doi: 10.1038/nature25167
11. He S, Sharpless NE. Senescence in health and disease. *Cell* (2017) 169(6):1000–11. doi: 10.1016/j.cell.2017.05.015
12. Collado M, Serrano M. Senescence in tumours: evidence from mice and humans. *Nat Rev Cancer* (2010) 10(1):51–7. doi: 10.1038/nrc2772
13. Petrova NV, Velichko AK, Razin SV, Kantidze OL. Small molecule compounds that induce cellular senescence. *Aging Cell* (2016) 15:999–1017. doi: 10.1111/acel.12518
14. You J, Dong R, Ying M, He Q, Cao J, Yang B. Cellular senescence and anti-cancer therapy. *Curr Drug Targets* (2019) 20(7):705–15. doi: 10.2174/1389450120666181217100833
15. Ou HL, Hoffmann R, González-López C, Doherty GJ, Korkola JE, Muñoz-Espin D. Cellular senescence in cancer: from mechanisms to detection. *Mol Oncol* (2021) 15(10):2634–71. doi: 10.1002/1878-0261.12807
16. Kumari R, Jat P. Mechanisms of cellular senescence: Cell cycle arrest and senescence associated secretory phenotype. *Front Cell Dev Biol* (2021) 9:645593. doi: 10.3389/fcell.2021.645593
17. Calcinotto A, Kohli J, Zagato E, Pellegrini L, Demaria M, Alimonti A. Cellular senescence: aging, cancer, and injury. *Physiol Rev* (2019) 99(2):1047–78. doi: 10.1152/physrev.00020.2018
18. Fane M, Weeraratna AT. How the ageing microenvironment influences tumour progression. *Nat Rev Cancer* (2020) 20(2):89–106. doi: 10.1038/s41568-019-0222-9
19. Yang L, Li C, Qin Y, Zhang G, Zhao B, Wang Z, et al. A novel prognostic model based on ferroptosis-related gene signature for bladder cancer. *Front Oncol* (2021) 11:686044. doi: 10.3389/fonc.2021.686044
20. Hu D, Jiang L, Luo S, Zhao X, Hu H, Zhao G, et al. Development of an autophagy-related gene expression signature for prognosis prediction in prostate cancer patients. *J Transl Med* (2020) 18(1):160. doi: 10.1186/s12967-020-02323-x
21. Casella G, Munk R, Kim KM, Piao Y, De S, Abdelmohsen K, et al. Transcriptome signature of cellular senescence. *Nucleic Acids Res* (2019) 47(14):7294–305. doi: 10.1093/nar/gkz555
22. Bussian TJ, Aziz A, Meyer CF, Swenson BL, van Deursen JM, Baker DJ. Clearance of senescent glial cells prevents tau-dependent pathology and cognitive decline. *Nature* (2018) 562:578–82. doi: 10.1038/s41586-018-0543-y
23. Eggert T, Wolter K, Ji J, Ma C, Yevsa T, Klotz S, et al. Distinct functions of senescence-associated immune responses in liver tumor surveillance and tumor progression. *Cancer Cell* (2016) 30:533–47. doi: 10.1016/j.ccell.2016.09.003
24. Prieto LI, Baker DJ. Cellular Senescence and the Immune System in Cancer. *Gerontology* (2019) 65(5):505–12. doi: 10.1159/000500683
25. Huang Z, Yan Y, Zhu Z, Liu J, He X, Dalangood S, et al. CBX7 suppresses urinary bladder cancer progression *via* modulating AKR1B10-ERK signaling. *Cell Death Dis* (2021) 12(6):537. doi: 10.1038/s41419-021-03819-0
26. Pallante P, Terracciano L, Carafa V, Schneider S, Zlobec I, Lugli A, et al. The loss of the CBX7 gene expression represents an adverse prognostic marker for survival of colon carcinoma patients. *Eur J Cancer* (2010) 46:2304–13. doi: 10.1016/j.ejca.2010.05.011
27. Karamitopoulou E, Pallante P, Zlobec I, Tornillo L, Carafa V, Schaffner T, et al. Loss of the CBX7 protein expression correlates with a more aggressive phenotype in pancreatic cancer. *Eur J Cancer* (2010) 46:1438–44. doi: 10.1016/j.ejca.2010.01.033
28. Pasquale EB. Eph receptors and ephrins in cancer: bidirectional signalling and beyond. *Nat Rev Cancer* (2010) 10(3):165–80. doi: 10.1038/nrc2806
29. Vail ME, Murone C, Tan A, Hii L, Abebe D, Janes PW, et al. Targeting EphA3 inhibits cancer growth by disrupting the tumor stromal microenvironment. *Cancer Res* (2014) 74(16):4470–81. doi: 10.1158/0008-5472.CAN-14-0218
30. Huang J, Teng L, Liu T, Li L, Chen D, Li F, et al. Identification of a novel serine/threonine kinase that inhibits TNF-induced NF- κ B activation and p53-induced transcription. *Biochem Biophys Res Commun* (2003) 309:774–8. doi: 10.1016/j.bbrc.2003.08.069
31. Maubant S, Tahtouh T, Brisson A, Maire V, Némati F, Tesson B, et al. LRP5 regulates the expression of STK40, a new potential target in triple-negative breast cancers. *Oncotarget* (2018) 9(32):22586–604. doi: 10.18632/oncotarget.25187
32. Lei XF, Fu W, Kim-Kaneyama JR, Omoto T, Miyazaki T, Li B, et al. Hic-5 deficiency attenuates the activation of hepatic stellate cells and liver fibrosis through upregulation of Smad7 in mice. *J Hepatol* (2016) 64:110–7. doi: 10.1016/j.jhep.2015.08.026
33. Arita-Okubo S, Kim-Kaneyama JR, Lei XF, Fu WG, Ohnishi K, Takeya M, et al. Role of hic-5 in the formation of microvilli-like structures and the monocyte-endothelial interaction that accelerates atherosclerosis. *Cardiovasc Res* (2015) 105:361–71. doi: 10.1093/cvr/cvv003
34. Gulvady AC, Dubois F, Deakin NO, Goreczny GJ, Turner CE. Hic-5 expression is a major indicator of cancer cell morphology, migration, and plasticity in three-dimensional matrices. *Mol Biol Cell* (2018) 29(13):1704–17. doi: 10.1091/mbc.E18-02-0092
35. Du X, Xu Q, Pan D, Xu D, Niu B, Hong W, et al. HIC-5 in cancer-associated fibroblasts contributes to esophageal squamous cell carcinoma progression. *Cell Death Dis* (2019) 10(12):873. doi: 10.1038/s41419-019-2114-z
36. Goreczny GJ, Ouderkerk-Pecone JL, Olson EC, Krendel M, Turner CE. Hic-5 remodeling of the stromal matrix promotes breast tumor progression. *Oncogene* (2017) 36(19):2693–703. doi: 10.1038/onc.2016.422
37. Sheta R, Wang ZQ, Bachvarova M, Plante M, Gregoire J, Renaud MC, et al. Hic-5 regulates epithelial to mesenchymal transition in ovarian cancer cells in a TGF β 1-independent manner. *Oncotarget* (2017) 8(47):82506–30. doi: 10.18632/oncotarget.19714
38. Sha L, Ma D, Chen C. Exosome-mediated hic-5 regulates proliferation and apoptosis of osteosarcoma *via* wnt/ β -catenin signal pathway. *Aging (Albany NY)* (2020) 12(23):23598–608. doi: 10.18632/aging.103546
39. Shao W, Espenshade PJ. Expanding roles for SREBP in metabolism. *Cell Metab* (2012) 16:414–9. doi: 10.1016/j.cmet.2012.09.002
40. Huang WC, Li X, Liu J, Lin J, Chung LW. Activation of androgen receptor, lipogenesis, and oxidative stress converged by SREBP-1 is responsible for regulating growth and progression of prostate cancer cells. *Mol Cancer Res* (2012) 10:133–42. doi: 10.1158/1541-7786.MCR-11-0206
41. Li LY, Yang Q, Jiang YY, Yang W, Jiang Y, Li X, et al. Interplay and cooperation between SREBF1 and master transcription factors regulate lipid metabolism and tumor-promoting pathways in squamous cancer. *Nat Commun* (2021) 12(1):4362. doi: 10.1038/s41467-021-24656-x
42. Wen YA, Xiong X, Zaytseva YY, Napier DL, Vallee E, Li AT, et al. Downregulation of SREBP inhibits tumor growth and initiation by altering cellular metabolism in colon cancer. *Cell Death Dis* (2018) 9(3):265. doi: 10.1038/s41419-018-0330-6
43. Dang CV. MYC on the path to cancer. *Cell* (2012) 149:22–35. doi: 10.1016/j.cell.2012.03.003
44. Duffy MJ, O'Grady S, Tang M, Crown J. MYC as a target for cancer treatment. *Cancer Treat Rev* (2021) 94:102154. doi: 10.1016/j.ctrv.2021.102154
45. Han H, Jain AD, Truica MI, Izquierdo-Ferrer J, Anker JF, Lysy B, et al. Small molecule MYC inhibitors suppress tumor growth and enhance immunotherapy. *Cancer Cell* (2019) 36(5):483–97. doi: 10.1016/j.ccell.2019.10.001
46. O'Donnell JS, Massi D, Teng MWL, Mandala M. PI3K-AKT-mTOR inhibition in cancer immunotherapy, redux. *Semin Cancer Biol* (2018) 48:91–103. doi: 10.1016/j.semcancer.2017.04.015
47. Larson C, Oronsky B, Carter CA, Oronsky A, Knox SJ, Sher D, et al. TGF- β : a master immune regulator. *Expert Opin Ther Targets* (2020) 24(5):427–38. doi: 10.1080/14728222.2020.1744568
48. Marozzi M, Parnigoni A, Negri A, Viola M, Vigetti D, Passi A, et al. Extracellular matrix remodeling, and proteostasis in tumor microenvironment. *Int J Mol Sci* (2021) 22(15):8102. doi: 10.3390/ijms22158102
49. Vitiello GA, Miller G. Targeting the interleukin-17 immune axis for cancer immunotherapy. *J Exp Med* (2020) 217(1):e20190456. doi: 10.1084/jem.20190456
50. Hynes RO, Naba A. Overview of the matrisome — an inventory of extracellular matrix constituents and functions. *Cold Spring Harb Perspect Biol* (2012) 4:a004903. doi: 10.1101/cshperspect.a004903
51. Szarvas T. Matrix metalloproteinase-7 as a marker of metastasis and predictor of poor survival in bladder cancer. *Cancer Sci* (2010) 101:1300–8. doi: 10.1111/j.1349-7006.2010.01506.x
52. Zhang G, Miyake M, Lawton A, Goodison S, Rosser CJ. Matrix metalloproteinase-10 promotes tumor progression through regulation of

- angiogenic and apoptotic pathways in cervical tumors. *BMC Cancer* (2014) 14:310. doi: 10.1186/1471-2407-14-310
53. Daza J, Charap A, Wiklund PN, Sfakianos JP. Role of the innate immune system in the development, progression, and therapeutic response of bladder cancer. *Eur Urol Focus* (2020) 6(4):650–2. doi: 10.1016/j.euf.2020.02.013
54. Gust KM, Rebhan K, Resch I, Shariat SF, Necchi A. Immune checkpoint inhibition in muscle-invasive and locally advanced bladder cancer. *Curr Opin Urol* (2020) 30(4):547–56. doi: 10.1097/MOU.0000000000000783
55. Sathe A, Nawroth R. Targeting the PI3K/AKT/mTOR pathway in bladder cancer. *Methods Mol Biol* (2018) 655:335–50. doi: 10.1007/978-1-4939-7234-0_23
56. Ruan H, Li Y, Wang X, Sun B, Fang W, Jiang S, et al. CRYAB inhibits migration and invasion of bladder cancer cells through the PI3K/AKT and ERK pathways. *Jpn J Clin Oncol* (2020) 50(3):254–60. doi: 10.1093/jco/hyz172
57. Benjamin DJ, Lyou Y. Advances in immunotherapy and the TGF- β resistance pathway in metastatic bladder cancer. *Cancers (Basel)* (2021) 13(22):5724. doi: 10.3390/cancers13225724
58. Chen Z, He S, Zhan Y, He A, Fang D, Gong Y, et al. TGF- β -induced transgelin promotes bladder cancer metastasis by regulating epithelial-mesenchymal transition and invadopodia formation. *EBioMedicine* (2019) 47:208–20. doi: 10.1016/j.ebiom.2019.08.012
59. Liang Y, Zhu F, Zhang H, Chen D, Zhang X, Gao Q, et al. Conditional ablation of TGF- β signaling inhibits tumor progression and invasion in an induced mouse bladder cancer model. *Sci Rep* (2016) 6:29479. doi: 10.1038/srep29479
60. Pappu R, Ramirez-Carrozzi V, Sambandam A. The interleukin-17 cytokine family: critical players in host defence and inflammatory diseases. *Immunology* (2011) 134:8–16. doi: 10.1111/j.1365-2567.2011.03465.x
61. Mikkola T, Almahmoudi R, Salo T, Al-Samadi A. Variable roles of interleukin-17F in different cancers. *BMC Cancer* (2022) 22(1):54. doi: 10.1186/s12885-021-08969-0
62. Doroudchi M, Saidi M, Malekzadeh M, Golmoghaddam H, Khezri A, Ghaderi A. Elevated IL-17A levels in early stages of bladder cancer regardless of smoking status. *Future Oncol* (2013) 9:295–304. doi: 10.2217/fon.12.180
63. Wang L, Yi T, Kortylewski M, Pardoll DM, Zeng D, Yu H. IL-17 can promote tumor growth through an IL-6-Stat3 signaling pathway. *J Exp Med* (2009) 206:1457–64. doi: 10.1084/jem.20090207
64. Rosenberg JE, Hoffman-Censits J, Powles T, van der Heijden MS, Balar AV, Necchi A, et al. Atezolizumab in patients with locally advanced and metastatic urothelial carcinoma who have progressed following treatment with platinum-based chemotherapy: a single-arm, multicentre, phase 2 trial. *Lancet* (2016) 387:1909–1920. doi: 10.1016/S0140-6736(16)00561-4
65. Balar AV, Galsky MD, Rosenberg JE, Thomas P, DP P, Joaquim B, et al. Atezolizumab as first-line treatment in cisplatin-ineligible patients with locally advanced and metastatic urothelial carcinoma: a single-arm, multicentre, phase 2 trial. *Lancet* (2017) 389:67–76. doi: 10.1016/S0140-6736(16)32455-2
66. Powles T, O'Donnell PH, Massard C, Arkenau HT, Friedlander TW, Hoimes CJ, et al. Efficacy and safety of durvalumab in locally advanced or metastatic urothelial carcinoma updated results from a phase 1/2 open-label study. *JAMA Oncol* (2017) 3:e172411. doi: 10.1001/jamaoncol.2017.2411
67. Sharma P, Callahan MK, Bono P, Kim J, Spiliopoulou P, Clvo E, et al. Nivolumab monotherapy in recurrent metastatic urothelial carcinoma (CheckMate 032): a multicentre, open-label, two-stage, multi-arm, phase 1/2 trial. *Lancet Oncol* (2016) 17:1590–1598. doi: 10.1016/S1470-2045(16)30496-X
68. Bellmunt J, de Wit R, Vaughn DJ, Fradet Y, Lee JL, Fong L, et al. Pembrolizumab as second-line therapy for advanced urothelial carcinoma. *N Engl J Med* (2017) 376:1015–1026. doi: 10.1056/NEJMoa1613683
69. Balar AV, Castellano D, O'Donnell PH, Grivas P, Vuky J, Powles T, et al. First-line pembrolizumab in cisplatin-ineligible patients with locally advanced and unresectable or metastatic urothelial cancer (KEYNOTE-052): a multicentre, single-arm, phase 2 study. *Lancet Oncol* (2017) 18:1483–1492. doi: 10.1016/S1470-2045(17)30616-2
70. Patel MR, Ellerton J, Infante JR, Agrawal M, Gordon M, Aljumailli R, et al. Avelumab in metastatic urothelial carcinoma after platinum failure (JAVELIN solid tumor): pooled results from two expansion cohorts of an open-label, phase 1 trial. *Lancet Oncol* (2018) 19:51–64. doi: 10.1016/S1470-2045(17)30900-2
71. Greten FR, Grivennikov SI. Inflammation and cancer: Triggers, mechanisms, and consequences. *Immunity* (2019) 51(1):27–41. doi: 10.1016/j.immuni.2019.06.025
72. Shalpour S, Karin M. Pas de deux: Control of anti-tumor immunity by cancer-associated inflammation. *Immunity* (2019) 51(1):15–26. doi: 10.1016/j.immuni.2019.06.021
73. Sun JX, Liu CQ, Xu JZ, An Y, Xu MY, Zhong XY, et al. A four-Cell-Senescence-Regulator-Gene prognostic index verified by genome-wide CRISPR can depict the tumor microenvironment and guide clinical treatment of bladder cancer. *Front Immunol* (2022) 13:908068. doi: 10.3389/fimmu.2022.908068
74. Zhou RR, Liang JJ, Tian H, Chen Q, Yang C, Liu CD. An immunosenescence-related gene signature to evaluate the prognosis, immunotherapeutic response, and cisplatin sensitivity of bladder cancer. *Dis Markers* (2022) 2022:2143892. doi: 10.1155/2022/2143892